EPMA IMAGES

The attached images and mineral data can be used to supplement an instrument-based lab, or serve as the basis for lab that can be completed without an instrument. Please provide credit for the images as given.

Figure 1. Principal beam-sample interactions. (a) Electron phenomena resulting from an impinging beam of electrons on a flat sample. (b) Electron-sample interactions within the "interaction volume", whose size depends on beam energy and sample characteristics (primarily average atomic number, or atomic density).

Additional diagrams to illustrate the schematics of a microprobe or SEM, ionization phenomena, electron shell structure, etc., can be found in Goldstein et al. (1992).

Figure 2. Secondary electron (SE) images. (a) Fossil diatoms. (b) Galena (PbS) crystals. Images courtesy Ellery Frahm, University of Minnesota Microprobe Lab.

Figure 3. Back-scattered electron (BSE) image of sample of pelitic schist from Antarctica. Field of view is approximately 5 mm. In general, brighter minerals have higher mean Z (where Z is atomic number).

Figure 4. X-ray composition maps collected by rastering the electron beam over an area of devitrified volcanic glass. BSE image (upper left) shows overall compositional variation as differences in mean Z. Remaining images show relative abundances of specific elements. Brighter areas reflect higher concentration. Images courtesy Ellery Frahm, University of Minnesota Microprobe Lab.

Figure 5. X-ray composition maps of plagioclase phenocrysts in volcanic glass, showing oscillatory growth zonation. Images courtesy Ellery Frahm, University of Minnesota Microprobe Lab.

Figure 6. X-ray composition maps of phenocrysts in volcanic glass, intergrown with magnetite grains. Images courtesy Ellery Frahm, University of Minnesota Microprobe Lab.

Figure 7. Thin section photomicrographs of sample 89GGR-33A, a pelitic schist from the Ross orogen, Transantarctic Mountains, Antarctica. Field of view is approximately 8 mm.

Figure 8. Back-scattered electron image map of a section of sample 89GGR-33A. Numbered circles correspond to spot locations where EDS spectra were collected.

Figure 9. Energy-dispersive spectra of spot mineral analyses in sample 89GGR-33A for locations 1-5 in Figure 8.

Figure 10. Energy-dispersive spectra of spot mineral analyses in sample 89GGR-33A for locations 6-10 in Figure 8.

Figure 11. Back-scattered and element composition maps for Area B of sample 89GGR-33A.

Figure 12. Element composition maps for Area C of sample 89GGR-33A.

Figure 13. Thin section photomicrographs of sample 89GGR-33B, an amphibolite from the Ross orogen, Transantarctic Mountains, Antarctica. Field of view is approximately 5 mm.

Figure 14. Back-scattered and element composition maps for a section of sample 89GGR-33B shown in Figure 13.

Figure 15. Energy-dispersive spectra of spot mineral analyses in sample 89GGR-33B for locations 1-4 in Figure 14.

ELECTRON PROBE ANALYSES

Mineral #1

SiO2	36.54
TiO2	0.03
Al2O3	20.76
MgO	3.39
CaO	1.22
MnO	0.41
∑Fe as FeO	37.69
Na2O	0.03
K2O	0.01

Mineral #5

SiO2	33.13
TiO2	3.48
Al2O3	17.73
MgO	5.95
CaO	0.02
MnO	0.01
∑Fe as FeO	23.93
Na2O	0.13
K2O	9.09

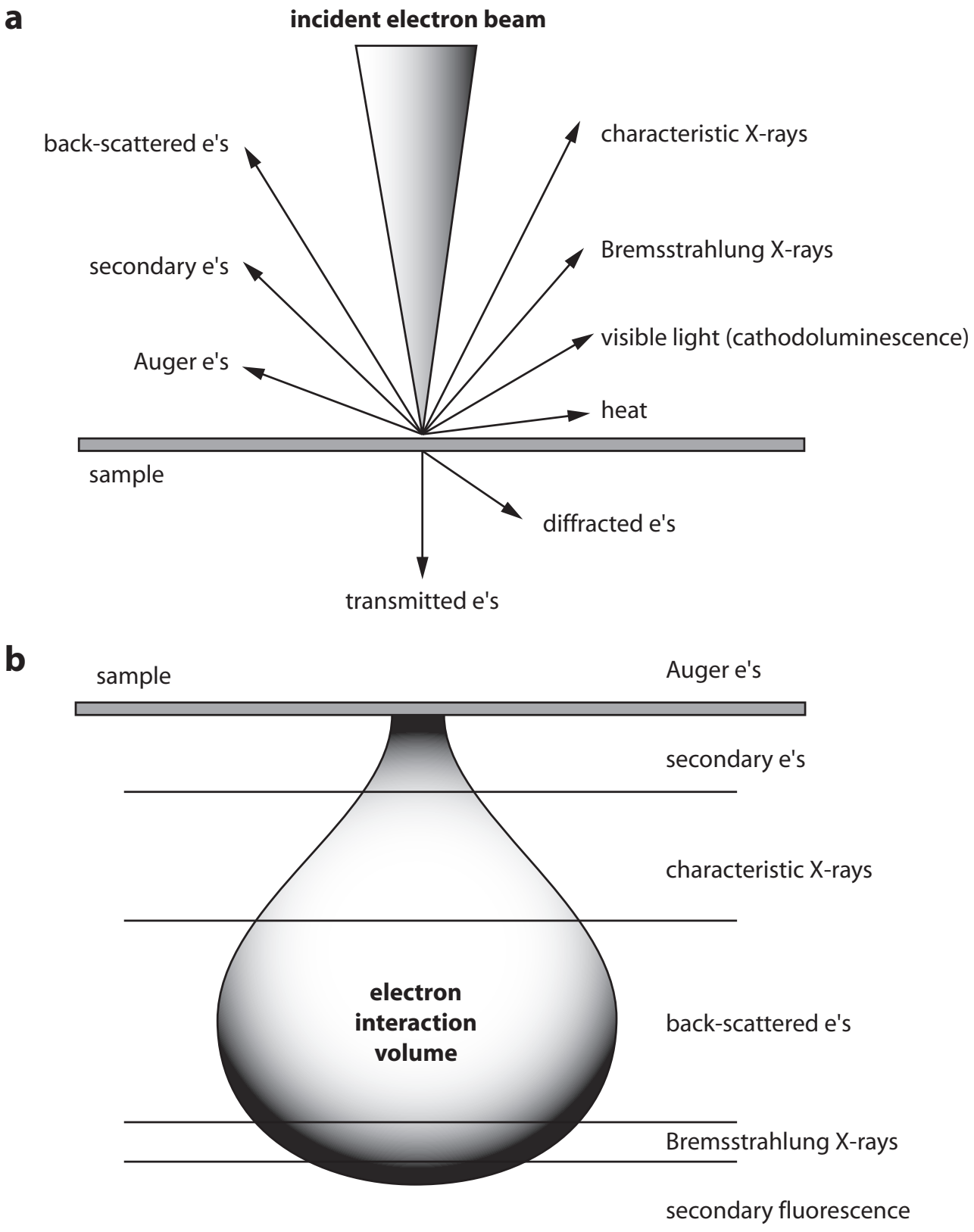

Figure 1. Principal beam-sample interactions. (a) Electron phenomena resulting from an impinging beam of electrons on a flat sample. (b) Electron-sample interactions within the "interaction volume", whose size depends on beam energy and sample characteristics

JWG 2003

SECONDARY ELECTRON (SE) IMAGES

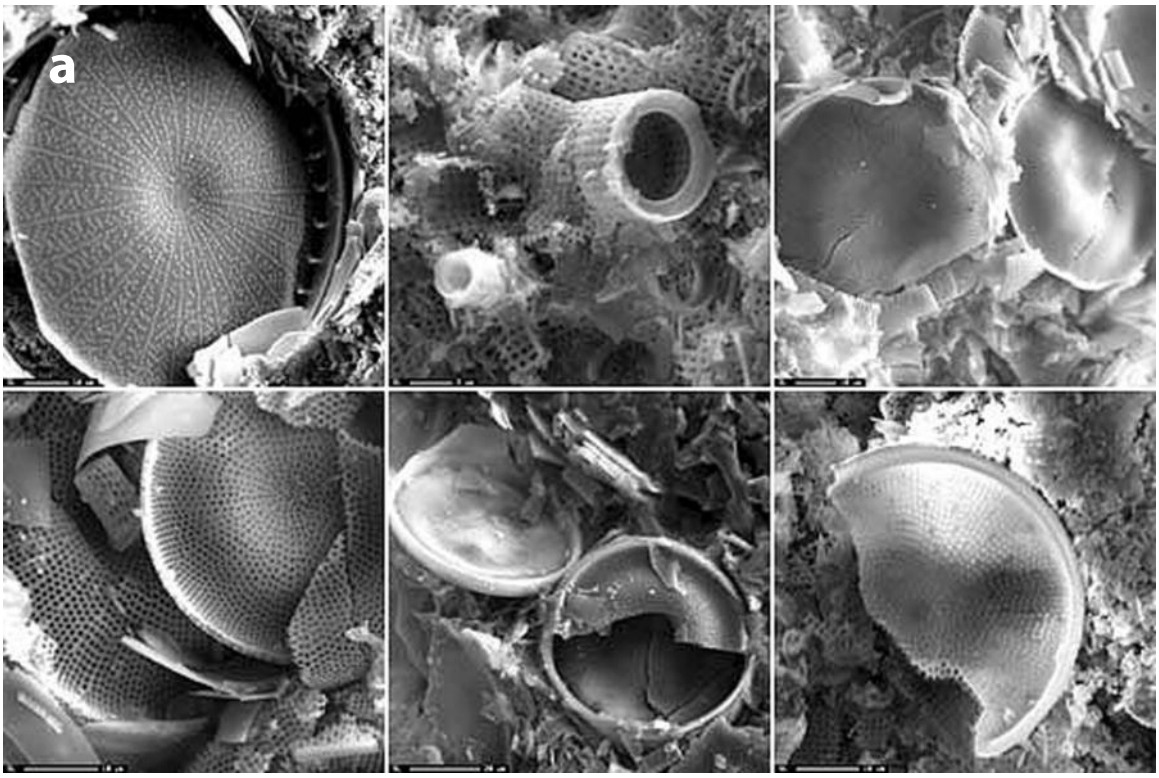

University of Minnesota microprobe lab (Analyst: Ellery Frahm)

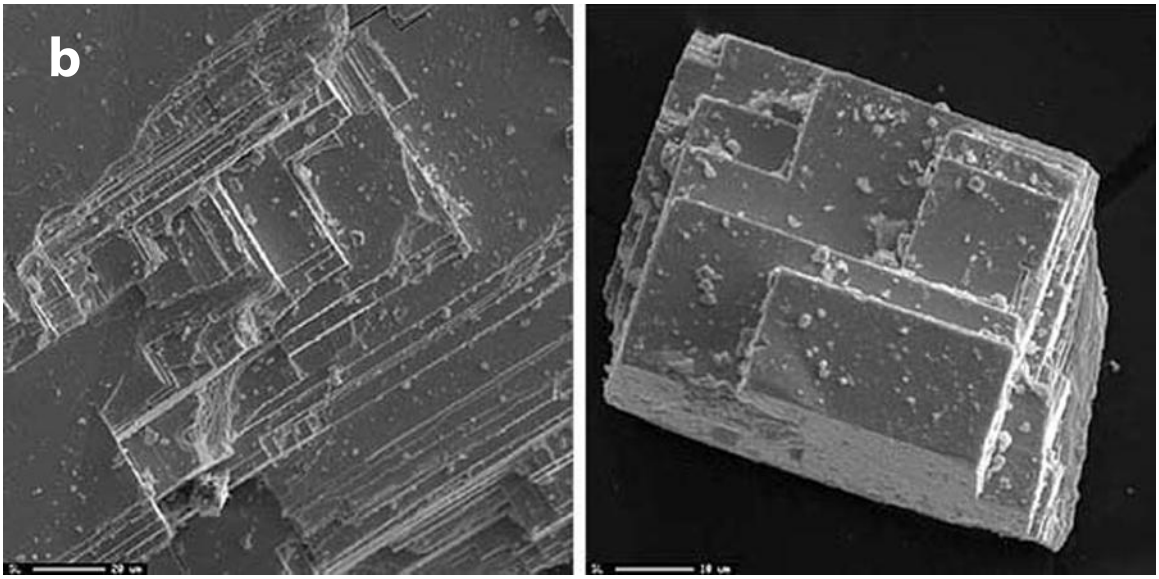

University of Minnesota microprobe lab (Analyst: Ellery Frahm)

Figure 2. Secondary electron (SE) images. (a) Fossil diatoms. (b) Galena (PbS) crystals. Images courtesy Ellery Frahm, University of Minnesota Microprobe Lab.

JWG 2003

BACK-SCATTERED ELECTRON (BSE) IMAGE

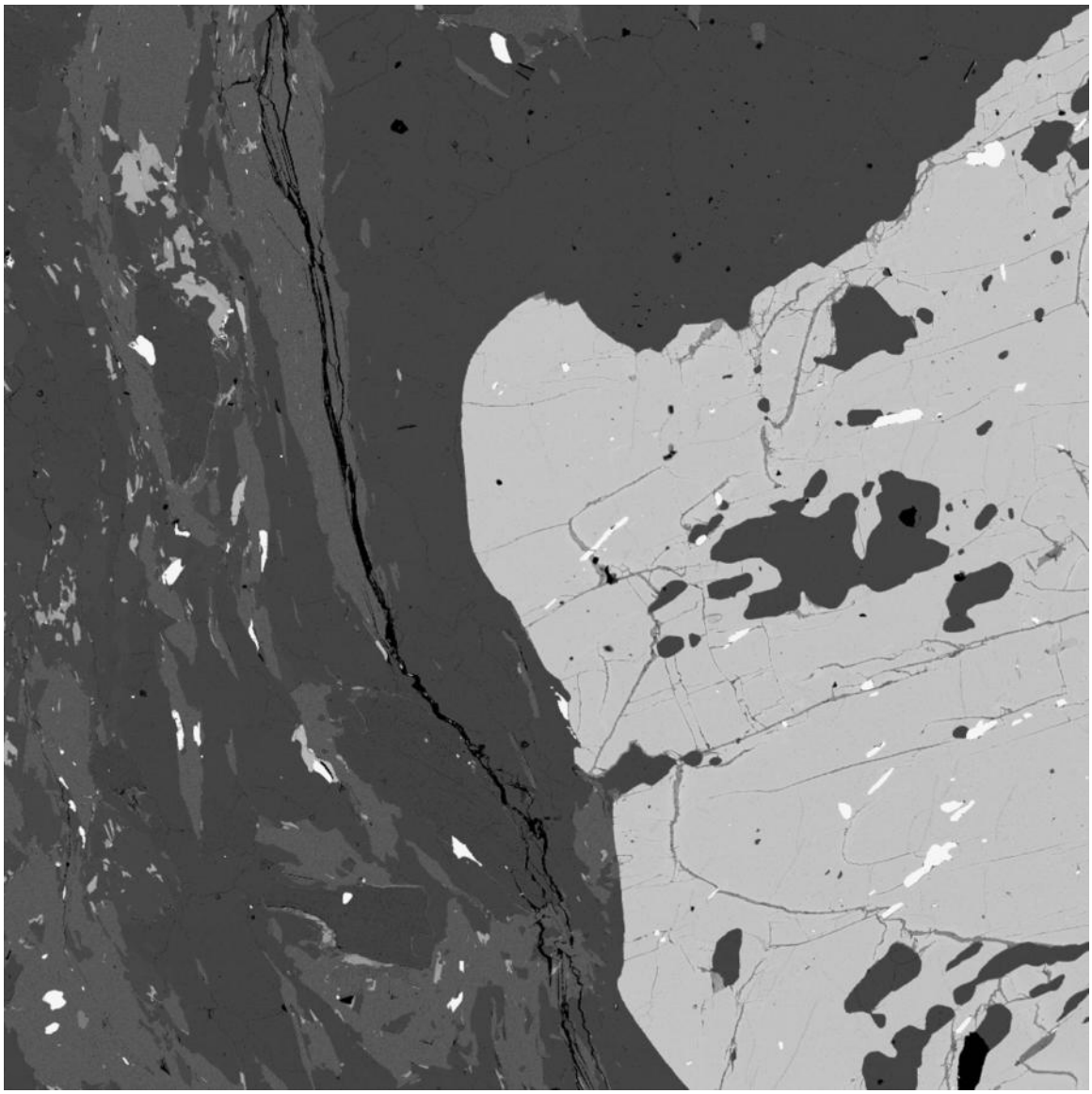

Figure 3. Back-scattered electron (BSE) image of sample of pelitic schist from Antarctica. Field of view is approximately 5 mm. In general, brighter minerals have higher mean Z (where Z is atomic number).

JWG 2003

X-ray COMPOSITION MAPS

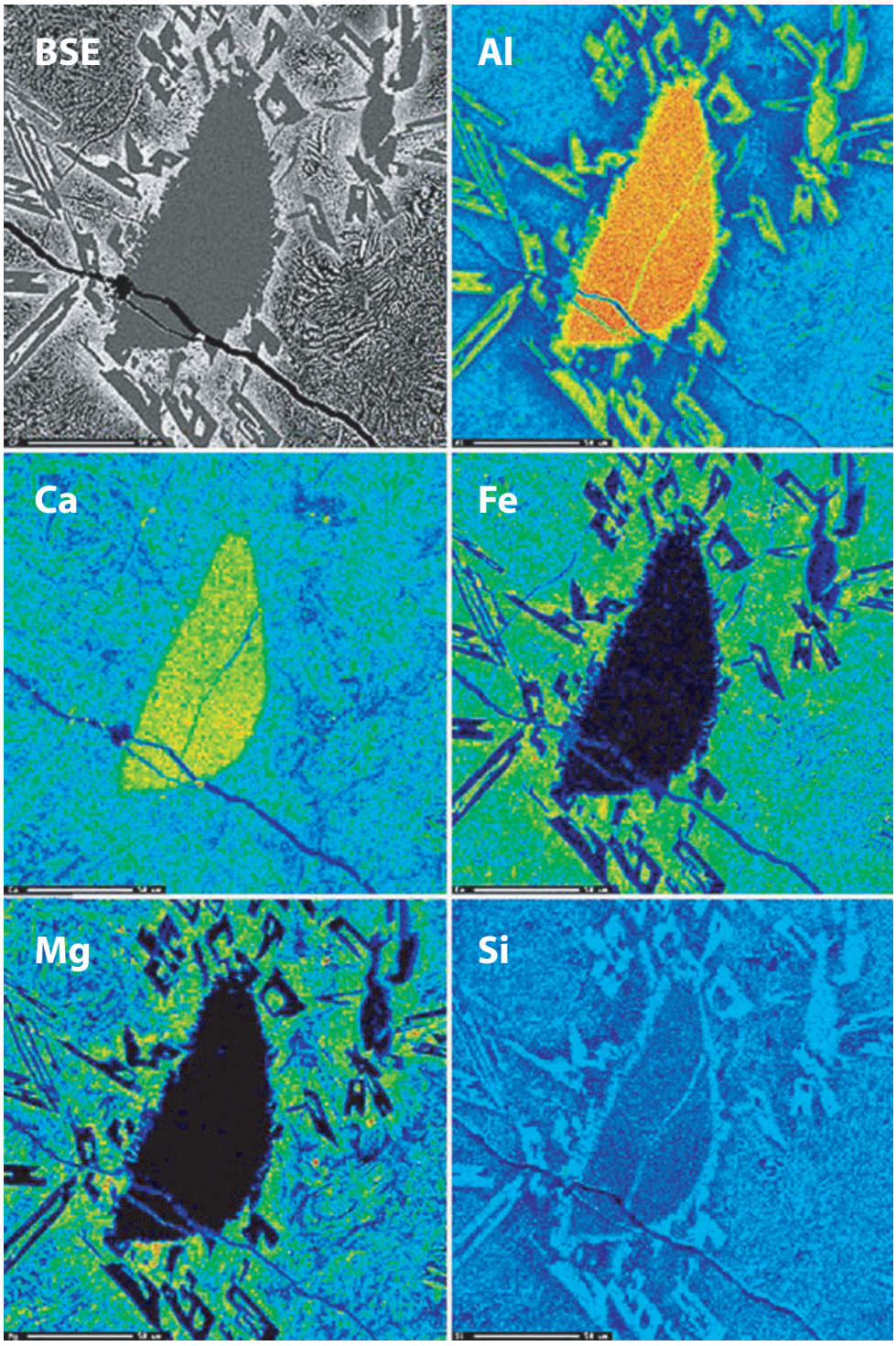

University of Minnesota microprobe lab (Analyst: Ellery Frahm)

Figure 4. X-ray composition maps collected by rastering the electron beam over an area of devitrified volcanic glass. BSE image (upper left) shows overall compositional variation as differences in mean Z. Remaining images show relative abundances of specific elements. Brighter areas reflect higher concentration.

JWG 2003

X-ray COMPOSITION MAPS

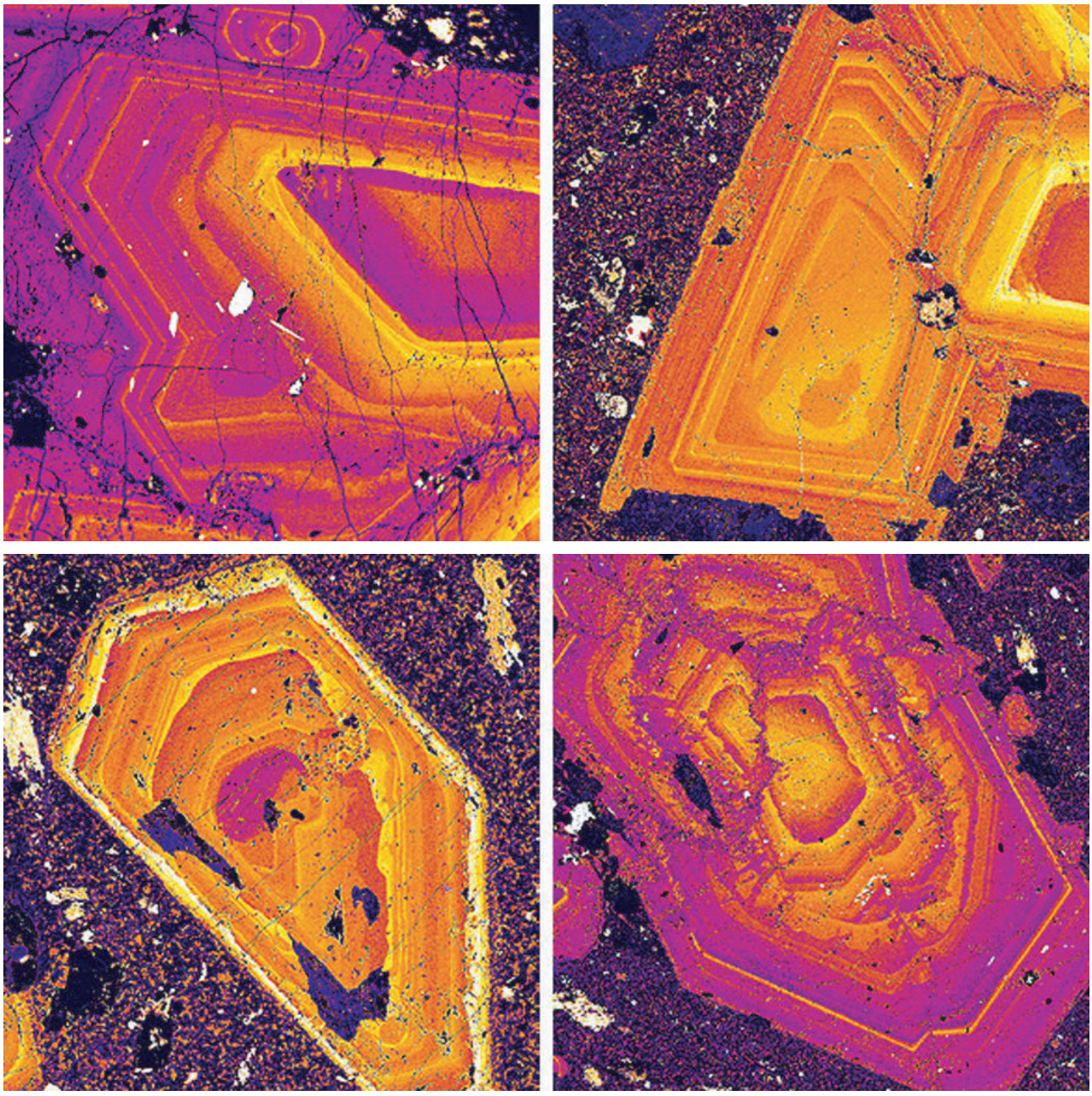

University of Minnesota microprobe lab (Analyst: Ellery Frahm)

Figure 5. X-ray composition maps of plagioclase phenocrysts in volcanic glass, showing oscillatory growth zonation.

JWG 2003

X-ray COMPOSITION MAPS

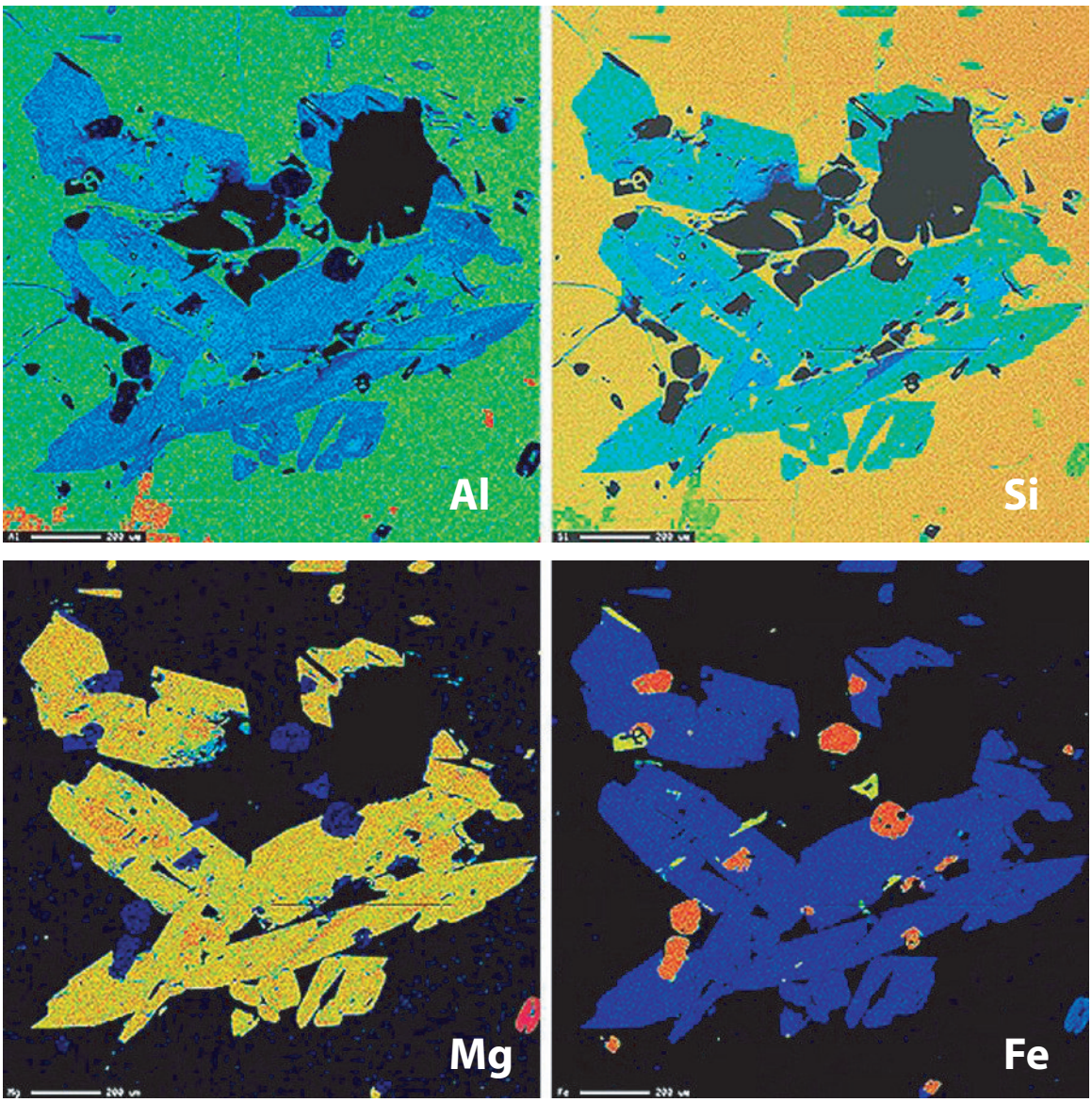

University of Minnesota microprobe lab (Analyst: Ellery Frahm)

Figure 6. X-ray composition maps of phenocrysts in volcanic glass, intergrown with magnetite grains.

JWG 2003

89GGR-33A

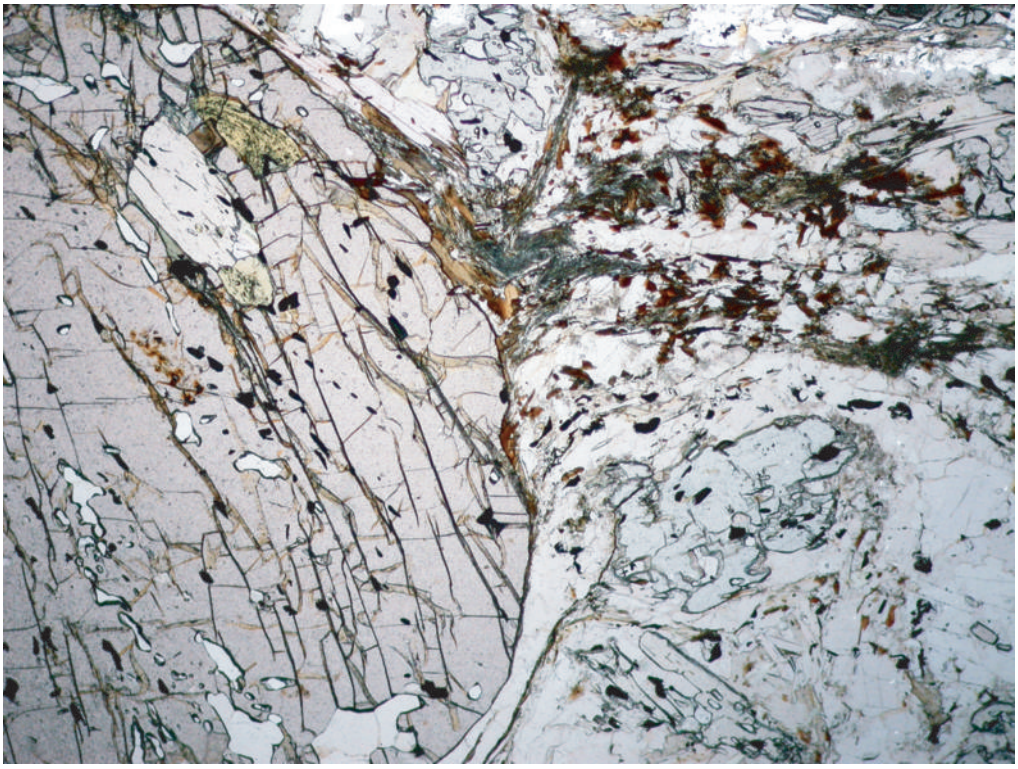

Plane-polarized light

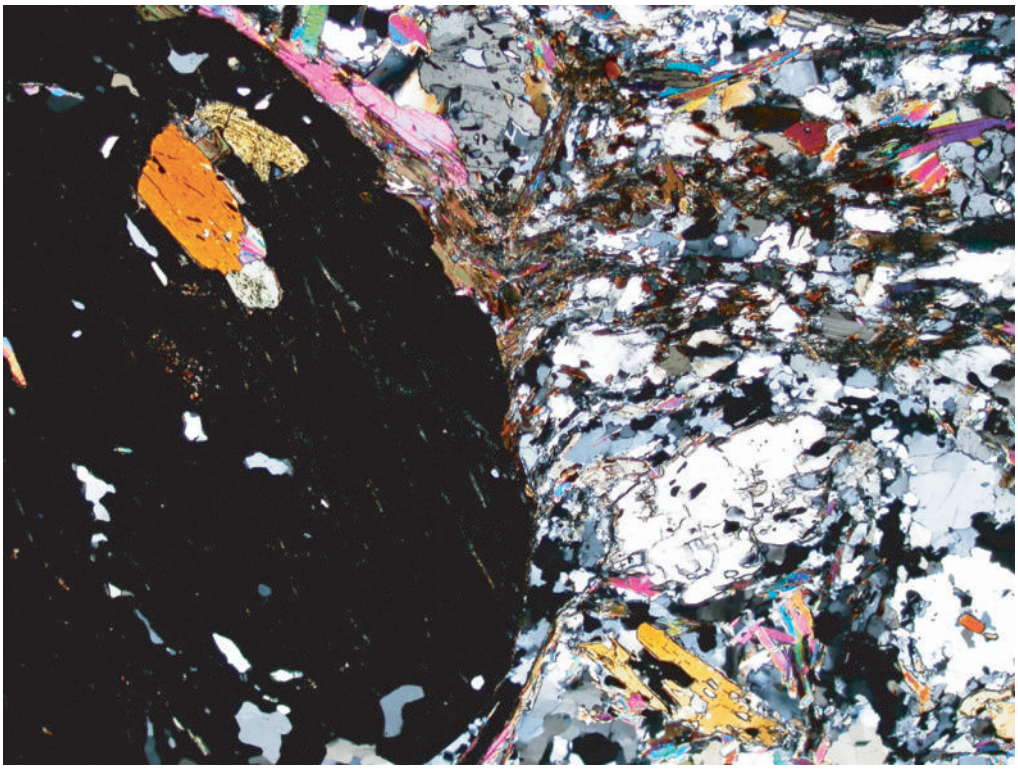

Crossed-polarized light

Figure 7. Thin section photomicrographs of sample 89GGR-33A, a pelitic schist from the Ross orogen, Transantarctic Mountains, Antarctica. Field of view is approximately 8 mm.

JWG 2003

89GGR-33A: BSE map

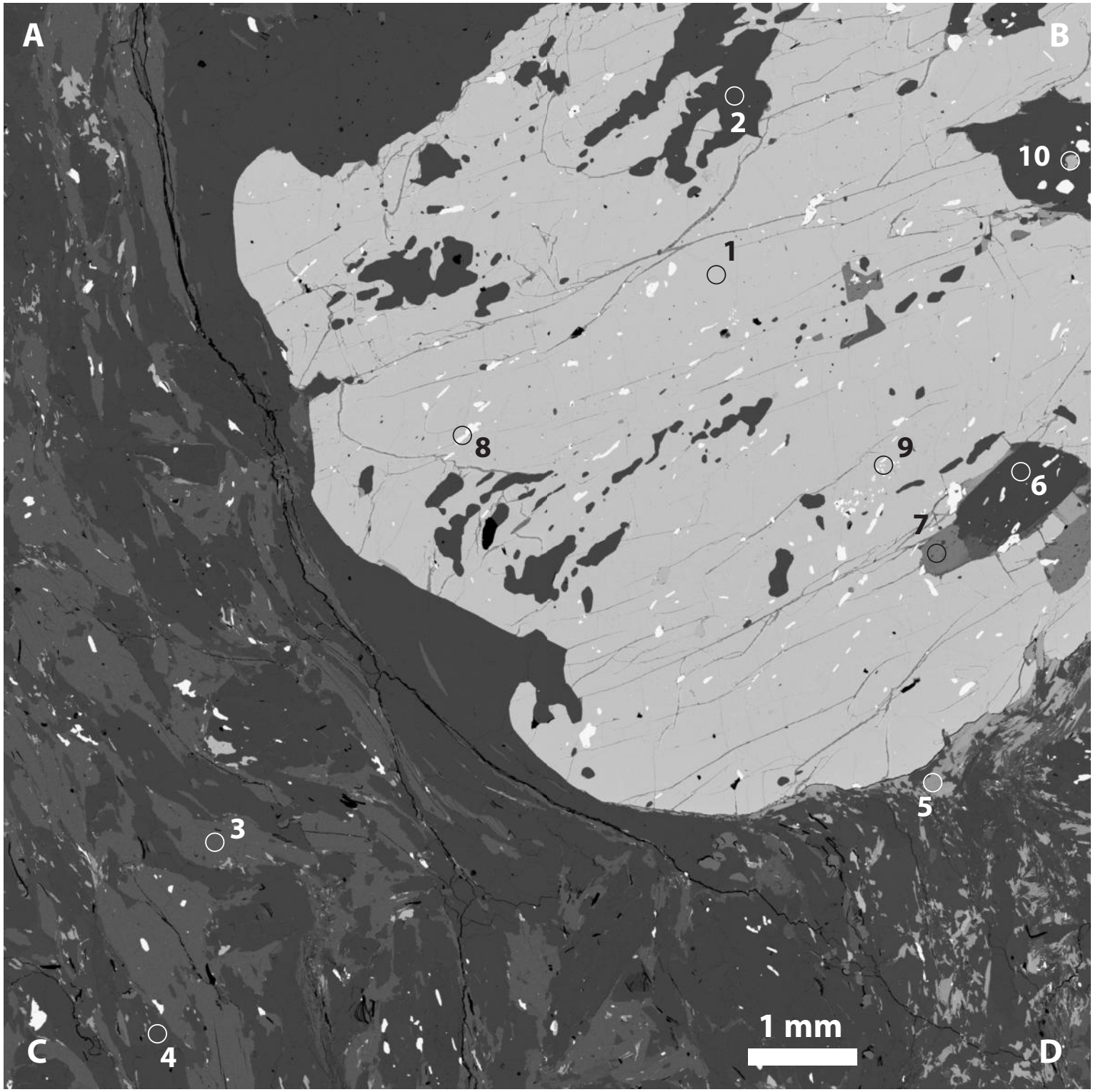

Figure 8. Back-scattered electron image map of a section of sample 89GGR-33A. Numbered circles correspond to spot locations where EDS spectra were collected.

JWG 2003

89GGR-33A

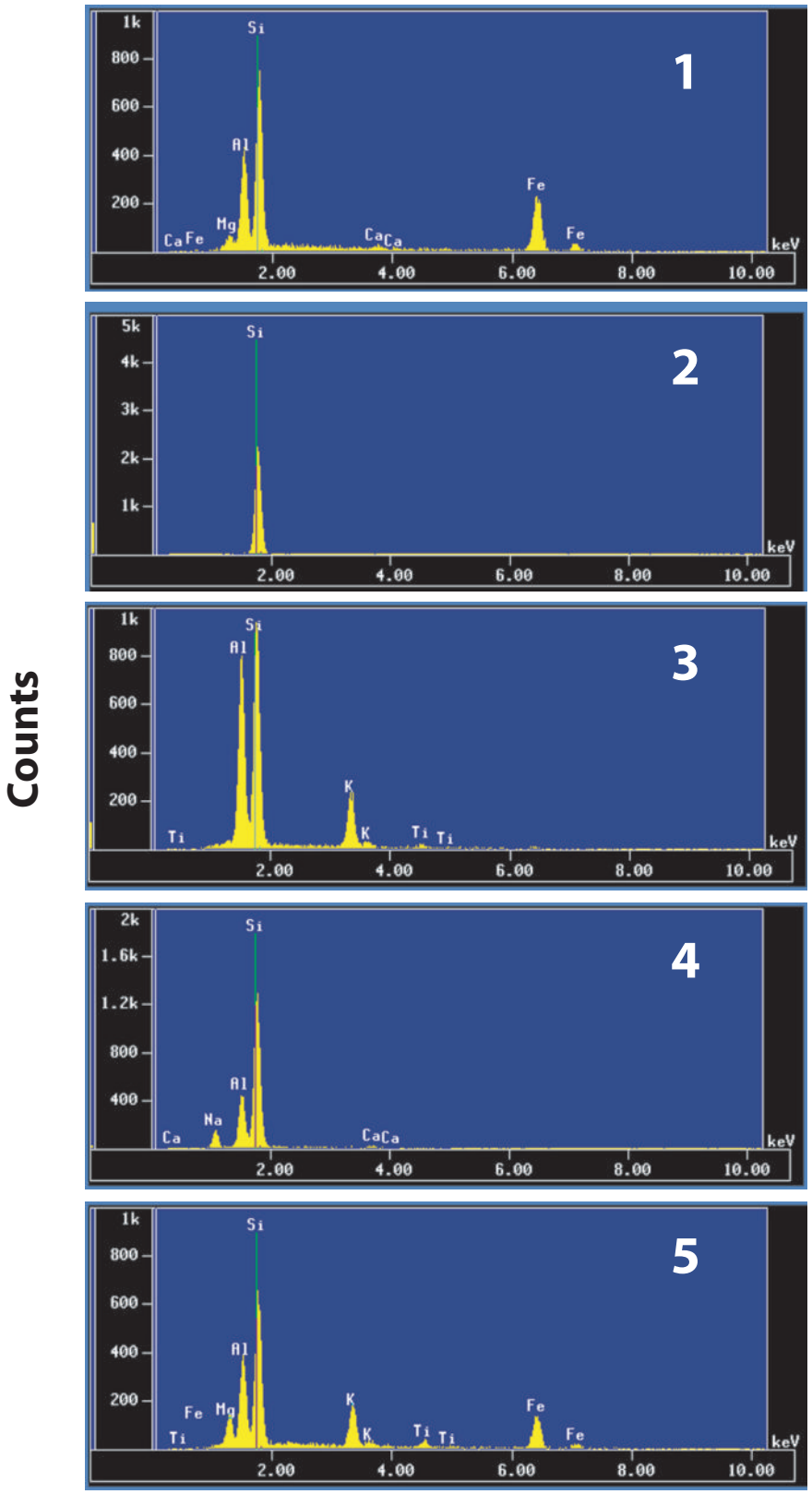

Figure 9. Energy-dispersive spectra of spot mineral analyses in sample 89GGR-33A for locations 1-5 in Figure 8.

JWG 2003

89GGR-33A

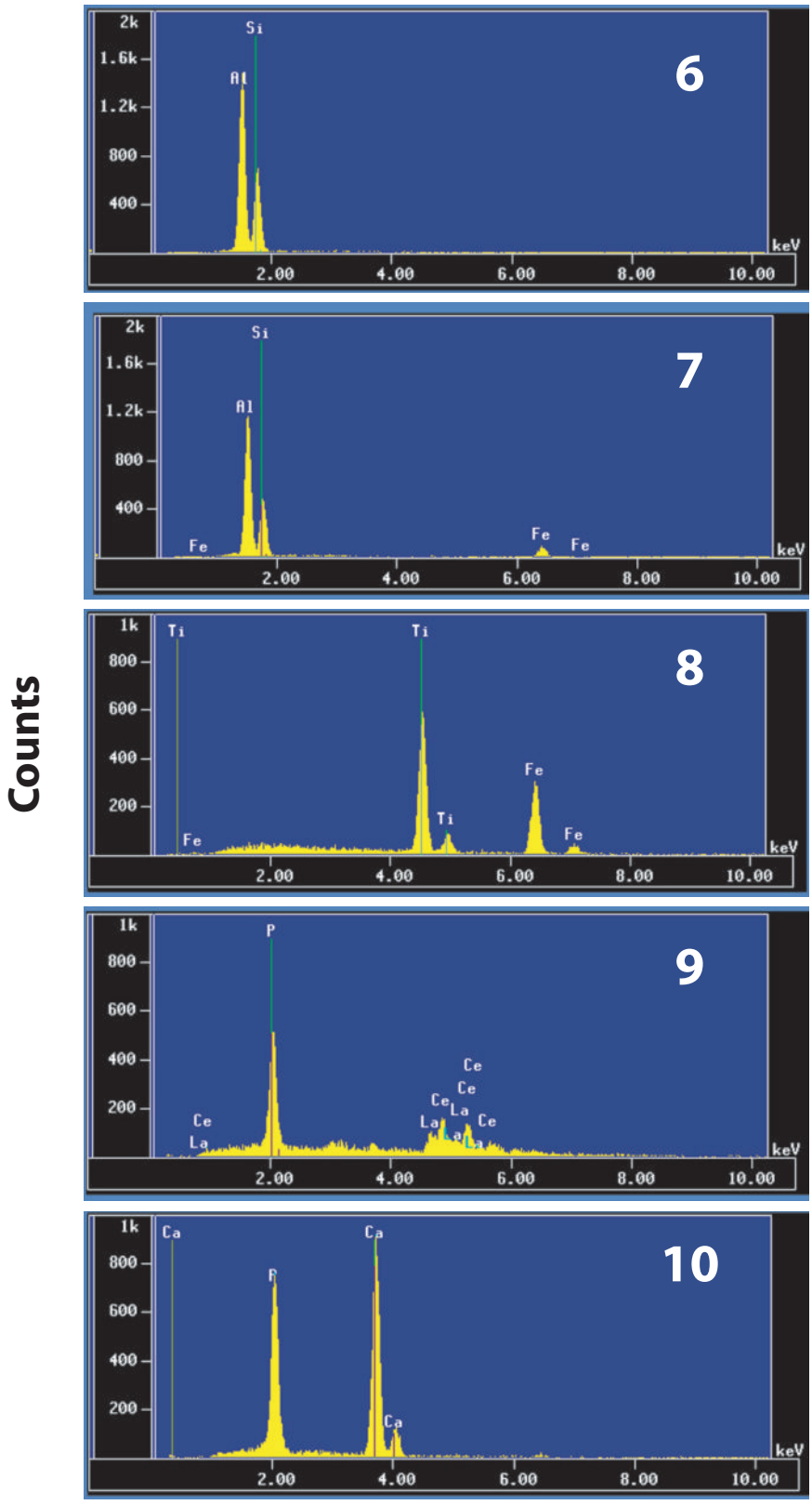

Energy (keV)

Figure 10. Energy-dispersive spectra of spot mineral analyses in sample 89GGR-33A for locations 6-10 in Figure 8.

JWG 2003

89GGR-33A (Area B)

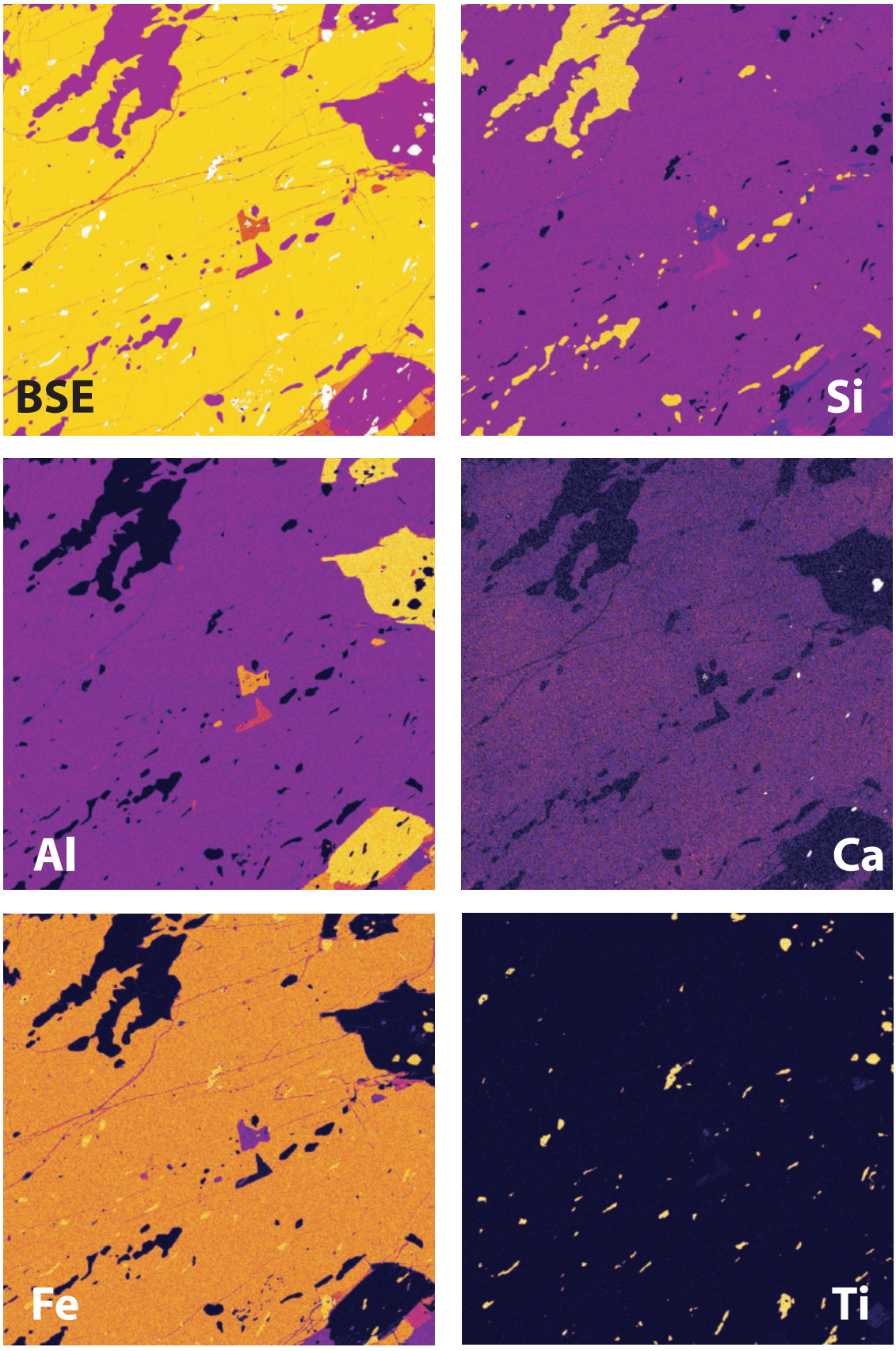

Figure 11. Back-scattered and element composition maps for Area B of sample 89GGR-33A.

JWG 2003

89GGR-33A (Area C)

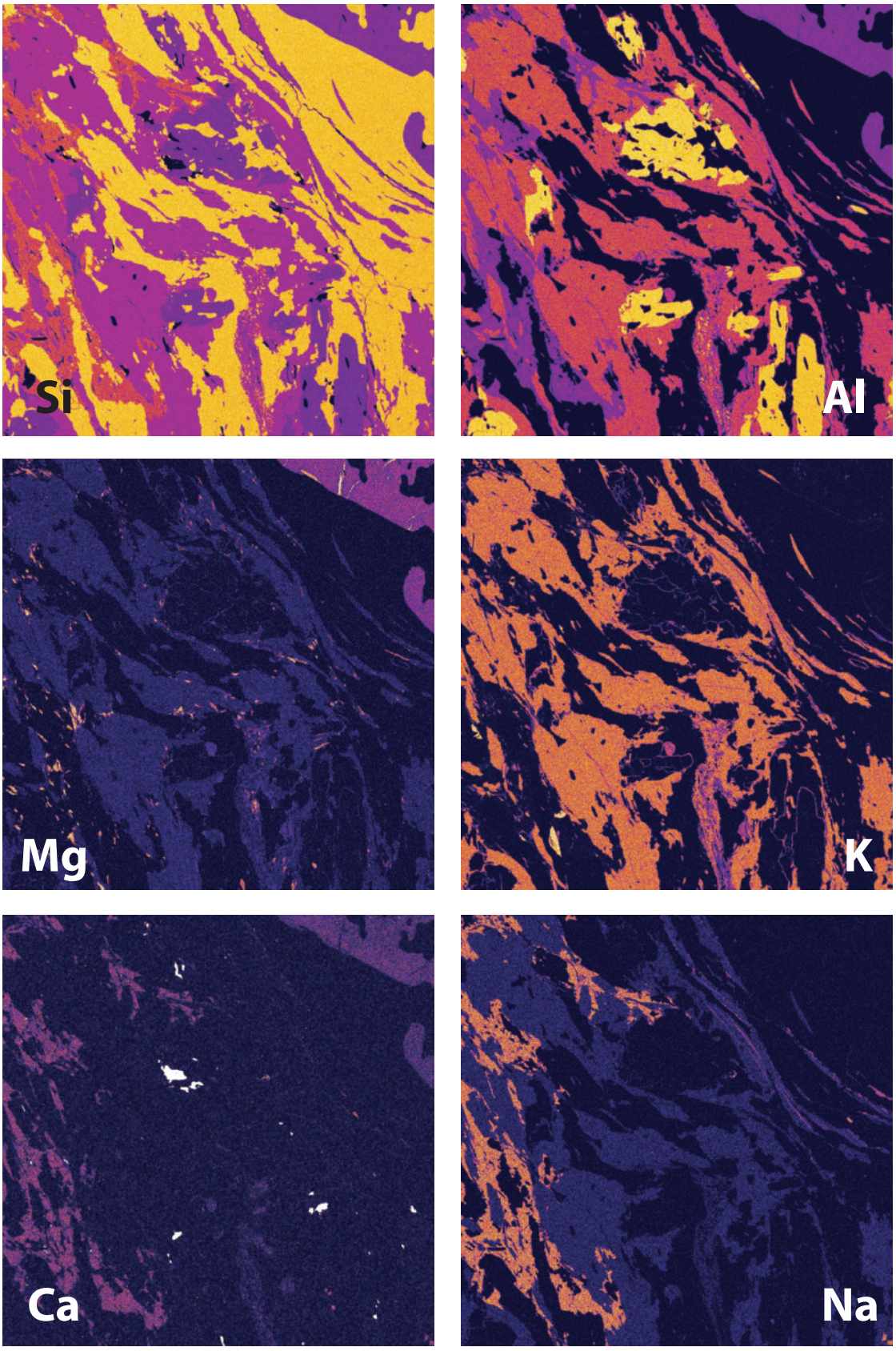

Figure 12. Element composition maps for Area C of sample 89GGR-33A.

JWG 2003

89GGR-33B

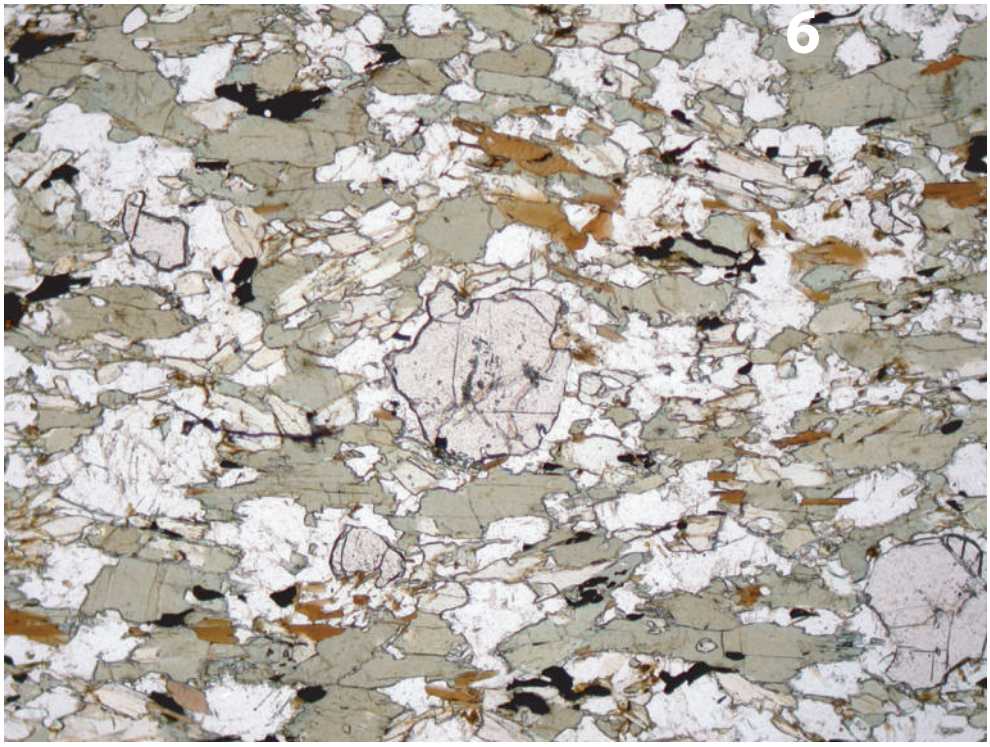

Plane-polarized light

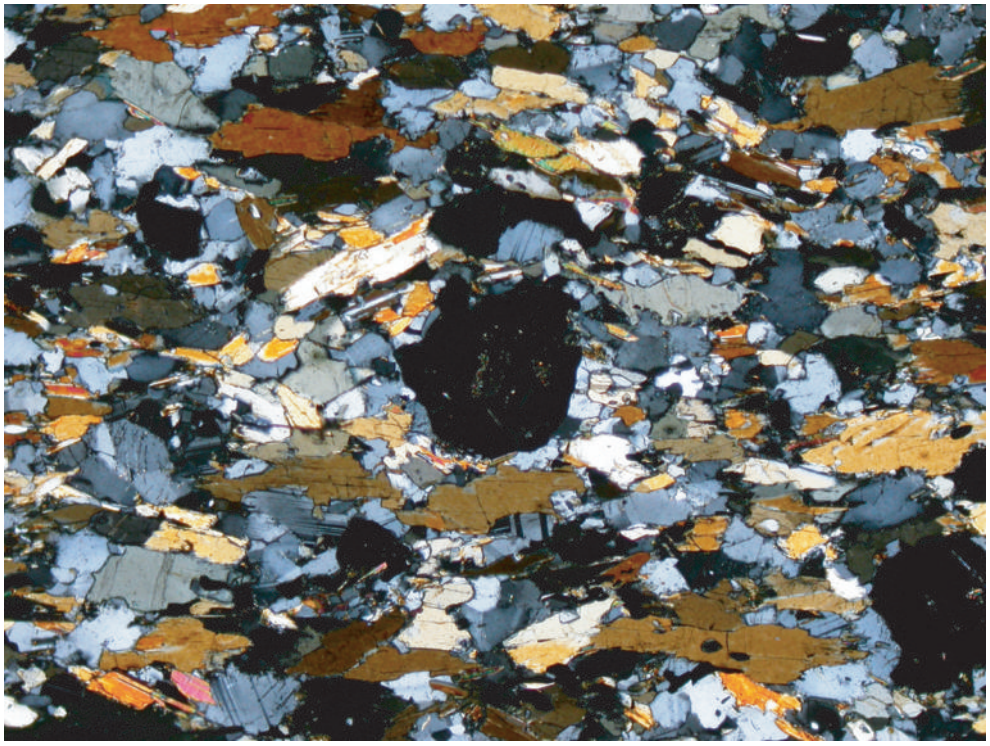

Crossed-polarized light

Figure 13. Thin section photomicrographs of sample 89GGR-33B, an amphibolite from the Ross orogen, Transantarctic Mountains, Antarctica. Field of view is approximately 5 mm.

JWG 2003

89GGR-33B

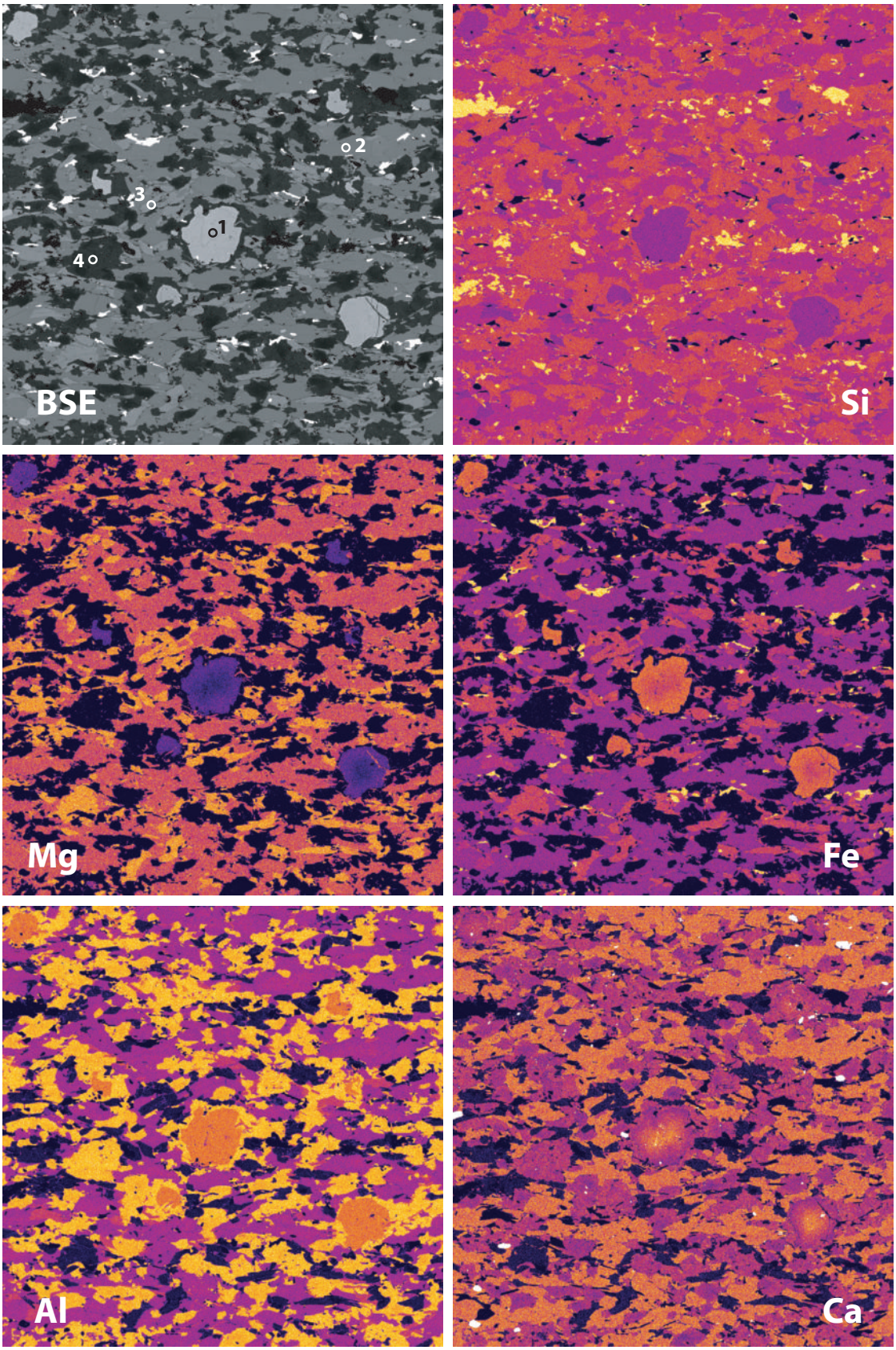

Figure 14. Back-scattered and element composition maps for a section of sample 89GGR-33B shown in Figure 13.

JWG 2003

89GGR-33B

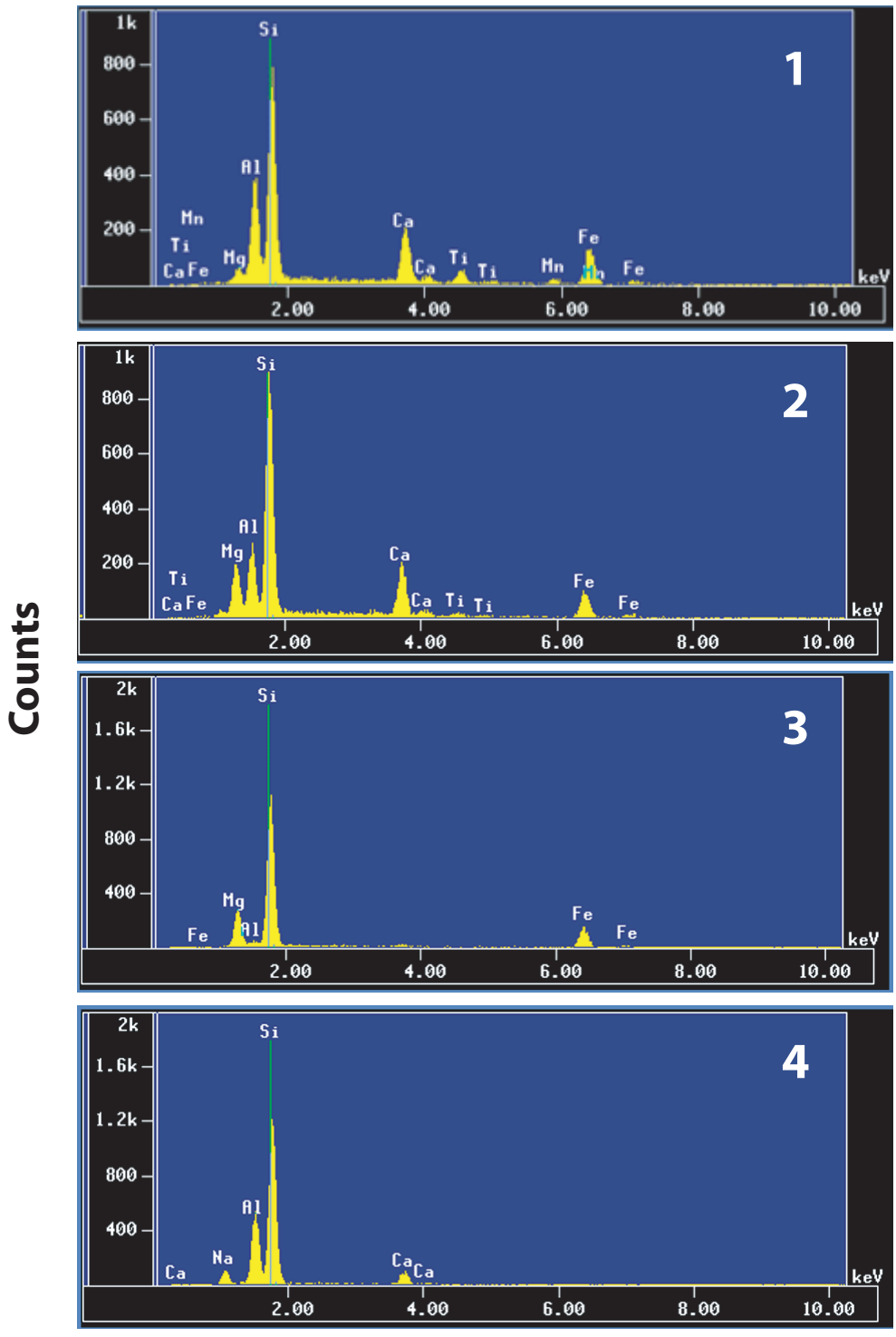

Figure 15. Energy-dispersive spectra of spot mineral analyses in sample 89GGR-33B for locations 1-4 in Figure 14.

JWG 2003